Cavity-enhanced atom detection with cooperative noise reduction

J. Goldwin,[1,2] M. Trupke, J. Kenner, A. Ratnapala,[1] and E. A. Hinds[1]

[1] *Centre for Cold Matter, Imperial College, Prince Consort Road, London SW7 2BW, United Kingdom*
[2] *School of Physics and Astronomy, University of Birmingham, Birmingham B15 2TT, United Kingdom*

(Dated: September 16, 2010)

An optical microcavity with small mode radius is used to measure the local density of a cold atom cloud. Atom densities below 1 per cavity mode volume are measured with signals near the photon shot-noise limit. Atom detection is fast and efficient, reaching fidelities in excess of 97% after $10\,\mu$s and 99.9% after $30\,\mu$s. Notably, the fluctuations of the detected photon counts are smaller than expected for Poissonian distributions of atoms probed with Poissonian light fields. This noise suppression is attributed to multi-atom effects on the collective atomic dipole interacting with the cavity field. Our measurements confirm a decade-old theory of atomic beams in cavity quantum electrodynamics.

High finesse optical resonators can improve the sensitivity of atom detection by increasing the lifetime of photons and confining them to a small volume [1]. Long photon lifetime, controlled by cavity length and mirror reflectivity, increases the effective optical thickness of an intra-cavity sample by a factor on the order of the finesse $\mathcal{F} \gg 1$. Small mode volume, which depends only on the geometry of the resonator, increases the energy density per photon and therefore the Einstein coefficients describing transition rates. Thus the spontaneous emission rate of an atom is increased by coupling it to a resonant cavity [2]. Importantly, all the additional photons are emitted into the cavity mode, making it possible to detect fluorescence even at very low atom density. For sufficiently small mode volumes, a single cavity photon becomes intense enough to saturate the atomic transition. In this regime vacuum fluctuations modify the spectral properties of the coupled atom-cavity system [3] in such a way as to allow detection at the single-atom level [4, 5].

Recently there has been growing interest in cold atom experiments with atomic density distributions extending throughout or beyond the range of the cavity field [6, 7]. For multiple atoms, the radiative behavior is collective [8]. Although the gas may be dilute, the common coupling to the electromagnetic field produces effective long-range interactions between the atoms that can lead to self-organization [9] and collective motion [10], as well as super-radiant Rayleigh scattering and collective atomic recoil lasing [11]. Recently experimenters have exploited these effects to realize a quantum phase transition from a Bose-Einstein condensate to a supersolid [12].

A central parameter in describing cavity-enhanced detection is the dimensionless single-atom cooperativity [13], $C_1 = g^2/(2\kappa\gamma)$, where $2\,g$ is the single-photon Rabi frequency at the peak of the cavity intensity distribution, $2\,\kappa$ is the cavity linewidth (full-width at half maximum), and $2\,\gamma$ the natural atomic linewidth. The cooperativity determines both the effect of a single atom on the cavity spectrum, and the rate of fluorescence into the cavity.

In the case of multiple atoms, the cooperativity is generalized by defining $C_N = C_1\,N_{\rm eff}$ where the effective atom number is [14]

$$N_{\rm eff} = \int_0^L \int_{-\infty}^{\infty}\int_{-\infty}^{\infty} |\chi(\mathbf{r})|^2 \varrho(\mathbf{r})\,{\rm d}^3\mathbf{r} \qquad (1)$$

with $\varrho(\mathbf{r})$ being the atomic density, L the cavity length, and $\chi(\mathbf{r}) = \sin(2\pi\,z/\lambda)\exp[-(x^2+y^2)/w^2]$ the cavity field mode function (λ is the wavelength). When the atom cloud is much larger than the cavity mode volume $V_{\rm cav} = \pi w^2 L/4$, the atom density is approximately uniform over the interaction region, and $\langle N_{\rm eff}\rangle \approx \varrho(0)\,V_{\rm cav}$. At low densities, single-atom physics dominates, while at higher densities multi-atom effects become important [14]. In this Letter we perform local density measurements on large dilute clouds of atoms in the crossover regime, paying particular attention to fluctuations. We show that even at densities on the order of one atom per cavity mode volume, the atomic shot noise is heavily suppressed by collective effects.

Our apparatus has been described in detail in Refs. [5, 15]. We work with ^{87}Rb, near the D_2 resonance at $\lambda = 780\,$nm. Our optical microcavity is formed between the end of a single-mode optical fiber and a spherical surface microfabricated in silicon, both being coated with dielectric mirrors. The resulting plano-concave cavity mode has a length of $L = 139(1)\,\mu$m and a waist whose e^{-1} field radius is $w = 4.46(7)\,\mu$m. To our knowledge the only Fabry-Perot cavity with a smaller mode waist is the all-fibre design of Ref. [7] ($w = 3.9\,\mu$m). Since $C_1 \propto \mathcal{F}/w^2$, a small waist makes it possible to detect single atoms using a cavity of relatively modest finesse. This relaxes the usual need for very high mirror quality and reduces the sensitivity to noise in the cavity length. For this work we have $g = 2\pi \times 98.4(1.6)\,$MHz, $\kappa = 2\pi \times 5200(100)\,$MHz, and $\gamma = 2\pi \times 3\,$MHz, giving $C_1 = 0.307(11)$. We begin each experimental sequence by cooling and trapping $\sim 2\times10^7$ ^{87}Rb atoms in a magneto-optical trap formed above a mirror [16], followed by sub-Doppler cooling to $16\,\mu$K in optical molasses. We then release the atoms, which fall through a hole in the mirror and pass through a cavity mounted immediately below.

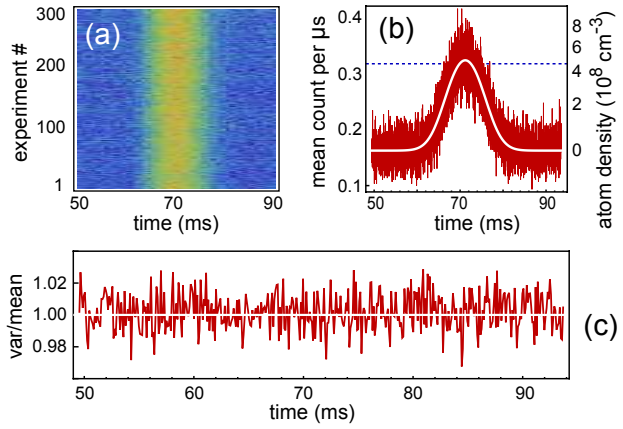

FIG. 1: Reflection measurements. (a) Detected photon counts for 300 identical experiments. The atoms are released at 39.5 ms. Counts increase from blue to red. Data were taken with 2 μs resolution, and the image was then re-binned to 1 ms. (b) The data in red are averages over the 300 drops shown in (a), while the white curve is a fit to Eq. (2) assuming a Gaussian dependence of C_N on time; the dashed blue line gives the value expected from a single atom maximally coupled to the cavity mode. (c) Ratio of ensemble variance to mean versus time. The red curve is calculated from the raw data in (a) for each 2 μs time bin, and then a 100 μs running average is applied to smooth the result; the white line is the photon shot-noise level.

As described in [5], we detect atoms either by (i) measuring changes in the intensity of a probe beam reflected from the cavity; or (ii) detecting fluorescence when exciting the atoms uniformly with a laser beam propagating transverse to the cavity axis. We refer to these simply as reflection and fluorescence measurements, respectively. If atoms are present and the cavity and lasers are resonant with the free-space atomic transition, then one can show [17] that the steady-state rate of photons travelling from the cavity to the detector is

$$J_{\rm out} = \begin{cases} J_{\rm in}\left(\dfrac{b+2\,C_N}{1+2\,C_N}\right)^2 & , \quad \text{reflection} \\ 2\,C'_N\,\gamma\,\xi\,\dfrac{s}{(1+2\,C'_N)^2+s} & , \quad \text{fluorescence} \end{cases} \tag{2}$$

where $J_{\rm in}$ is the number of incident probe photons per second and b^2 characterizes the reflection fringe contrast in the absence of atoms. The cooperativities in reflection (C_N) and fluorescence (C'_N) are not generally the same since they depend on the polarization of the probe light and the excitation light respectively. In fluorescence, $s = \frac{1}{2}(\Omega/\gamma)^2$ is the free-space saturation parameter for excitation driven at a Rabi frequency Ω, while ξ is the probability for an intracavity photon to pass from the cavity into the fiber [18]. Finally we have used the facts that $(g/\kappa)^4 \ll 1$, and that the atomic excited state fraction is small in our reflection measurements.

Figure 1(a) shows the results of repeated reflection measurements as the cloud falls through the cavity. A circularly-polarized probe drives the atomic cycling transition, maximizing the atom-field coupling strength. At early and late times, there are no atoms in the cavity, so the reflected light is at its minimum value, determined by the incident probe power and the empty cavity fringe contrast. The reflected intensity rises when there are atoms in the cavity. These experimental runs are averaged in Figure 1(b), which also shows a fit to the evolution expected from Eq. (2) with a peak $\langle N_{\rm eff}\rangle = 1.06(4)$, corresponding to only $4.9(2)\times10^8$ atoms cm^{-3}. For reference, the dashed line shows the expected reflection with a single atom maximally coupled to the cavity mode. Note that the 10 ms width of the curve reflects the size of the cloud, which is determined by its temperature. By contrast, the typical transit time for a single atom passing through the width of the cavity mode is $\sim 14\,\mu$s, so the cloud is very large compared with the extent of the cavity field. In Fig. 1(c) we plot as a function of time the variance of the photon counts divided by the mean, evaluated over the 300 repetitions of the experiment. This ratio is strikingly close to 1, indicating that the noise is dominated by photon shot-noise, regardless of whether the atoms are present or not. This is surprising as one might have expected relatively large atomic shot noise at such low effective atom number, as in Ref. [19]. We will return to this below, when we see a similar noise suppression in our fluorescence measurements.

Figure 2(a) shows the fluorescence signal. As the cloud falls through the cavity we switch on a resonant excitation beam whose (downward) propagation direction and polarization are both perpendicular to the cavity axis. The photon count rate immediately jumps to a high level as a result of the laser-induced fluorescence. Independent reflection measurements determine that the initial $\langle N_{\rm eff}\rangle = 1.24(5)$. Although the atom number is nearly constant over several ms during the reflection measurements, the signal here decays roughly exponentially with a time constant of order 100 μs. This is because the atoms are heated and pushed out of the cavity by the excitation light [17], which is much more intense than the probe light used in reflection measurements. In Fig. 2(b) we plot how the variance of the fluorescence count over 250 repetitions varies with the mean number of counts. Once again, we see that the fluctuations are very near the photon shot-noise limit, which is indicated by the solid line.

To calculate the expected noise level for our fluorescence signal, let us first apply the methods of Ref. [20]. Atomic motion is negligible over the 1 μs time bin of a single measurement, so we consider each measurement to have a fixed number of atoms N, producing a Poissonian photon count k with mean αN (the background is negligible). Since N fluctuates over repeated experiments, the photon counts obey $\mathrm{Var}(k)/\langle k\rangle = 1 + \alpha\mathrm{Var}(N)/\langle N\rangle$. If atoms are positioned randomly with a uniform probabil-

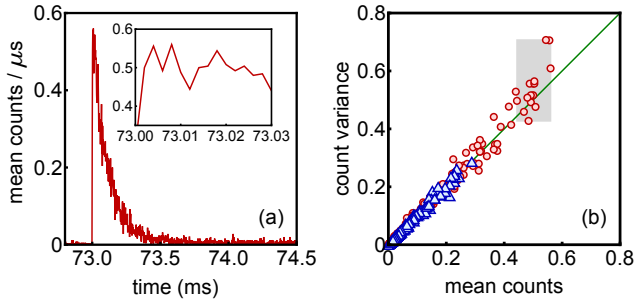

FIG. 2: Fluorescence measurements. (a) Fluorescence pulse, averaged over 250 drops. The exciting laser is pulsed on after the peak atomic density has passed through the cavity. At the start of the pulse, shown in detail in the inset, $\langle N_{\rm eff}\rangle = 1.24(5)$. This is slightly larger than in Fig. 1 due to a higher atom number in the initial MOT. (b) Variance of fluorescence counts as a function of mean. Red circles are from the data used in (a), and blue triangles are from a set where the drive beam is pulsed on at a later time in the drop, with initial $\langle N_{\rm eff}\rangle = 0.50(2)$. The green line is the photon shot-noise limit. The grey box corresponds to the inset in (a).

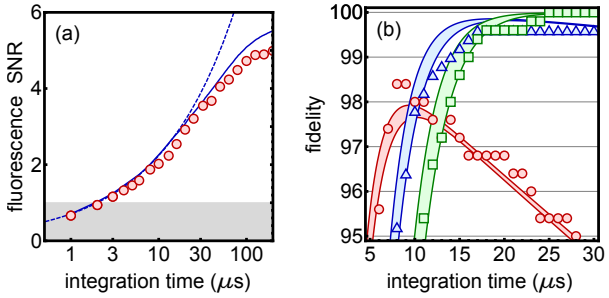

FIG. 3: Signal-to-noise ratio (SNR) and detection fidelity. Points are derived from the same data that were used to make Fig. 2(a). (a) Fluorescence SNR versus integration time. The solid curve is $\langle k\rangle^{1/2}$. The dashed curve shows $\langle k\rangle^{1/2}$ for constant $\langle N_{\rm eff}\rangle$. (b) Detection fidelity $F_K(\tau)$ for $K = 1$, 2, and 3 counts (○, △, and □). Points are from 500 measurements with $p = 1/2$ and curves show Eq. (3), assuming Poisson distributions with mean signal and background count rates obtained from the data at the beginning of the pulse.

ity distribution, the number of atoms in a given volume follows a Poisson distribution, and $\mathrm{Var}(N) = \langle N\rangle$. If we simply replace N with $N_{\rm eff}$, then we would expect $\mathrm{Var}(k)/\langle k\rangle = 1.40(3)$ for our experiment, which is well above the observed value of 1.09(3).

However when dealing with noise, N and $N_{\rm eff}$ are not interchangeable. The correct description of our fluctuations requires the full multi-atom probability distribution for $N_{\rm eff}^{1/2}$, which has been derived by Carmichael and Sanders [14]. From their work we find that $\mathrm{Var}(N_{\rm eff})/\langle N_{\rm eff}\rangle = 3/8$ in the limits of low and high atom density; numerically this appears to remain true for intermediate densities. Furthermore, C_N should be treated as a random variable proportional to $N_{\rm eff}$, rather than a constant proportional to $\langle N_{\rm eff}\rangle$, making α dependent on $N_{\rm eff}$. In practice this has only a small effect on $\langle k\rangle$, but is important for $\mathrm{Var}(k)$ because $J_{\rm out}$ saturates with large instantaneous values of $N_{\rm eff}$. When these effects are properly accounted for, we calculate $\mathrm{Var}(k)/\langle k\rangle = 1.095(8)$, in excellent agreement with our observed value. Furthermore, we note that a similar treatment of the reflection measurements in Fig. (1) gives $\mathrm{Var}(k)/\langle k\rangle = 1.005(2)$, consistent with the value 1.002(4) from the data. We therefore conclude that the full distribution of $N_{\rm eff}$ must be taken into account, and that the statistical nature of the collective atomic dipole leads to strong noise suppression in our experiments.

The signal-to-noise ratio (SNR) is $(\langle k\rangle - \langle k_{\rm bg}\rangle)/[\mathrm{Var}(k) + \mathrm{Var}(k_{\rm bg})]^{1/2}$, where k ($k_{\rm bg}$) is the number of photon counts with (without) atoms. Since the mean number of counts increases linearly with the duration τ of the photon-counting time bin we expect SNR $\propto \tau^{1/2}$ for our nearly Poissonian signal. In Fig. 3(a) we bin the fluorescence data to produce increasingly long measurement times and plot the result. At short times, this exhibits the expected behavior, with SNR $\approx (0.50\,\tau/\mu\mathrm{s})^{1/2}$. At longer times the SNR is reduced as $\langle N_{\rm eff}\rangle$ decreases due to scattering from the excitation laser.

It is also useful to discuss the discrete problem of detecting the presence (logical 1) or absence (logical 0) of an atom cloud. Because the fluctuations are dominated by noise in the photon number (as opposed to the atom number), this is equivalent in the case when $\langle N_{\rm eff}\rangle = 1$ to the problem of determining whether a single trapped atom fluoresces (logical 1) or not (logical 0), which is relevant for quantum information processing [21]. Our measurements at $\langle N_{\rm eff}\rangle = 1.24(5)$ imply a mean photon count rate at $\langle N_{\rm eff}\rangle = 1$ of $S(1) = 420(20)\,\mathrm{ms}^{-1}$. Table I shows that this is high in comparison with other atom detection experiments. Following [20], we could define the single-atom efficiency of the detector as $\eta = 1 - \exp[-S(1)\tau]$, which is the probability of counting ≥ 1 photon during the measurement time τ, assuming an atom is present and Poisson statistics with negligible background. This rises rapidly with our high count rate, reaching 98.5(3)% in only 10 μs.

Ref.	$S(1)$	B	$F_{1\max}, \tau_{1\max}$	$F_{2\max}$
[20]	5.6	0.28	90.9, 544	97.5
[19]	36	0.311	97.6, 132	99.8
[22]	54.5	2.18	92.2, 60	98.1
[23]	0.13	0.05	72.1, 9853	80.5
This work	420(20)	3.84(6)	97.46(13), 11.2(4)	99.79(2)

TABLE I: Comparison with other experiments. Rates are in cts/ms, fidelities in percent, and $\tau_{1\max}$ in μs. Note that $\tau_{K\max} = K\,\tau_{1\max}$ for $p = 1/2$. References [20, 22] use cavities, while Refs. [19, 23] use optical waveguides without cavities.

For most applications, however, it is not enough to detect logical 1 efficiently; the detector must also be able to identify logical 0 correctly. A more useful figure of merit is thus the fidelity, *i.e.* the probability of a correct measurement result. Let us take the detection of $\geq K$ photons as indicating logical 1, and $< K$ as logical 0. Then for Poissonian distributions the single-photon fidelity is $F_{K=1} = (1-p)\,e^{-B\tau} + p\,[1 - e^{-(S+B)\tau}]$, where B is the background photon counting rate and p is the probability that the state being measured is logical 1. The first (second) term is the probability of having logical 0 (1) and identifying it correctly. The blue curve in Fig. 3(b) shows the expected value of F_1 in our experiment over a data set for which $\langle N_{\rm eff}\rangle = 1.24$ and $p = 1/2$. The fidelity rises quickly as the detection of logical 1 becomes increasingly successful, but eventually falls due to false positives from the background. Superimposed on this curve are our measured values of the fidelity versus detection time, which agree well with our expectations. In general the maximum fidelity $F_{1\rm max}$ increases with S/B, reaching its peak at a time $\tau_{1\rm max}$ proportional to $1/S$ for fixed S/B. Table I compares our values of $F_{1\rm max}$ and $\tau_{1\rm max}$ with those for other atom detection experiments. Our detection reaches the best previous fidelity [19] and does so ten times more quickly.

A simple way to improve the fidelity is to increase the coincidence threshold K. This leads to the general result

$$F_K = (1-p)\,\frac{\Gamma[K, B\tau]}{(K-1)!} + p\left[1 - \frac{\Gamma[K,(B+S)\tau]}{(K-1)!}\right] \quad (3)$$

where $\Gamma[K,a]$ is the incomplete gamma function. These fidelities are plotted in Fig. 3(b) versus measurement time τ for the cases of $K = 2$ and 3. They peak at 99.79% and 99.98% when $\tau = 22.4\,\mu$s and $33.6\,\mu$s respectively. The data points again show that our measurements are consistent with expectations. Similar methods were exploited in [22], where two photons were required within a short time window in order to register a logical 1 result. With a $1\,\mu$s detection window they found that $99.719(6)\,\%$ of observed 2-photon coincidences were due to atoms, and described this percentage as the fidelity. In that experiment however, there was only a $0.2\,\%$ chance that the logical 1 state would produce a 2-photon count in the detection window. Thus, although their detection was very confident it was also very inefficient, having a low fidelity in the usual sense that we adopt here.

In conclusion we have characterized a new cavity-enhanced atom detector with low noise and high transverse spatial resolution. We have shown that the multi-atom nature of the collective atomic dipole results in a strong suppression of the atomic shot noise in approximately uniform systems. Our detector is fast and efficient, and suitable for detecting dilute samples below the level of a single atom per mode volume. Although we have focused here on measurements of low atomic densities, the dynamic range can be extended upwards simply by detuning the cavity and/or the probe field. We envision a variety of applications for making local density measurements on quantum gases. For example, there is sustained interest in studying the shell structure of Mott insulators in the Bose-Hubbard model [24], and our system would be ideal for studies of quantum transport of small impurities such as the recent work in Ref. [25].

We thank J. Dyne for technical expertise, and S. Barrett for an introduction to quantum jump theory and simulations. This work was funded by EPSRC and the Royal Society, and EU grants SCALA and AQUTE.

[1] J. Ye, and T. W. Lynn, in *Advances in Atomic, Molecular and Optical Physics, Vol. 49*, edited by B. Bederson and H. Walther (Elsevier, New York, 2003).
[2] E. M. Purcell, Phys. Rev. **69**, 681 (1946).
[3] E. E. Jaynes, and F. W. Cummings, Proc. of the IEEE **51**, 89 (1963).
[4] R. J. Thompson, G. Rempe, and H. J. Kimble, Phys. Rev. Lett. **68**, 1132 (1992); J. J. Childs et al. *ibid.* **77**, 2901 (1996); P. Münstermann et al. *ibid.* Phys. Rev. Lett. **84**, 4068 (2000).
[5] M. Trupke et al. Phys. Rev. Lett. **99**, 063601 (2007).
[6] F. Brennecke et al. Nature (London) **450**, 268 (2007); S. Gupta et al., Phys. Rev. Lett. **99**, 213601 (2007); I. Teper et al., Phys. Rev. A **78**, 051803(R) (2008); M. H. Schleier-Smith, I. D. Leroux, and V. Vuletić, Phys. Rev. Lett. **104**, 073604 (2010).
[7] Y. Colombe et al. Nature (London) **450**, 273 (2007).
[8] R. H. Dicke, Phys. Rev. **93**, 99 (1954); M. Tavis and F. W. Cummings, *ibid.* **170**, 379 (1968).
[9] H. W. Chan, A. T. Black, and V. Vuletić, Phys. Rev. Lett. **90**, 063003 (2003); A. T. Black, H. W. Chan, and V. Vuletić, *ibid.* **91**, 203001 (2003).
[10] B. Nagorny, Th. Elsässer, and A. Hemmerich, Phys. Rev. Lett. **91**, 153003 (2003).
[11] S. Slama et al. Phys. Rev. Lett. **98**, 053603 (2007).
[12] K. Baumann et al., Nature (London) **464**, 1301 (2010).
[13] P. Horak et al. Phys. Rev. A **67**, 043806 (2003).
[14] H. J. Carmichael and B. C. Sanders, Phys. Rev. A **60**, 2497 (1999).
[15] M. Trupke et al. Appl. Phys. Lett. **87**, 211106 (2005).
[16] J. Reichel, W. Hänsel, and T. W. Hänsch, Phys. Rev. Lett. **83**, 3398 (1999).
[17] J. Kenner, Ph.D thesis, Imperial College London, 2010.
[18] M. Trupke, Ph.D thesis, Imperial College London, 2007.
[19] M. Wilzbach et al. Opt. Lett. **34**, 259 (2009).
[20] I. Teper, Y.-J. Lin, and V. Vuletić, Phys. Rev. Lett. **97**, 023002 (2006).
[21] J. Bochmann et al. Phys. Rev. Lett. **104**, 203601 (2010); R. Gehr et al. *ibid* **104**, 203602 (2010).
[22] M. L. Terraciano et al. Nat. Phys. **5**, 480 (2009).
[23] M. Kohnen et al. e-print *arXiv:0912.4460* (2009).
[24] S. Folling et al. Phys. Rev. Lett. **97**, 060403 (2006); G. K. Campbell et al. Science **313**, 649 (2006); N. Gemelke et al., Nature (London) **460**, 995 (2009); J. F. Sherson et al. *ibid.* **467** 68 (2010).
[25] S. Palzer et al., Phys. Rev. Lett. **103**, 150601 (2009).